coatings

MDPI

Communication

Preparation and Thermal Characterization of Hollow Graphite Fibers/Paraffin Composite Phase Change Material

Liyong Wang [1], Zhanjun Liu [2,3,*], Quangui Guo [2,3,*], Huiqi Wang [1,*], Xianglei Wang [4], Xiaozhong Dong [5], Xiaodong Tian [2] and Xiaohui Guo [2]

1 School of Energy and Power Engineering, North University of China, Taiyuan 030001, China; nucc@nuc.edu.cn
2 CAS Key Laboratory of Carbon Materials, Institute of Coal Chemistry, Chinese Academy of Sciences, Taiyuan 030001, China; tianxiaodong@sxicc.ac.cn (X.T.); guoxh@sxicc.ac.cn (X.G.)
3 Center of Materials Science and Optoelectronics Engineering, University of Chinese Academy of Sciences, Beijing 100049, China
4 Department of Chemical Engineering, Ordos Institute of Technology, Ordos 017000, China; wxl19830403@aliyun.com
5 Department of Materials Engineering, Taiyuan Institute of Technology, Taiyuan 030001, China; dongxzsx@163.com
* Correspondence: zjliu03@sxicc.ac.cn (Z.L.); qgguo@sxicc.ac.cn (Q.G.); hqiwang@nuc.edu.cn (H.W.)

Abstract: Paraffin is one of the most common and promising phase change materials to store and release thermal energy. The inadequacy of paraffin lies in its low thermal conductivity, which affects its further application on thermal energy storage. In this work, hollow fibers derived from pitch were spun. The graphitization (treated at 2773 K under argon atmosphere) induced the carbon atom arrangement and lattice order development, which endowed the hollow graphite fibers (HGFs) with good graphite structure. The HGFs applied as thermal additives into paraffin significantly improved its thermal conductivity. The high thermal conductivity of the HGFs/paraffin composite was achieved up to 2.50 W/(m·K) along the fiber axis, which displayed an over 680% enhancement as compared with that of the pure paraffin. The HGFs displayed significant improvement of the heat transfer rate and heat flow of paraffin, which indicated the promising potential application of the HGFs/paraffin PCM in thermal energy storage systems.

Keywords: hollow graphite fibers; paraffin; phase change materials; thermal conductivity

check for updates

Citation: Wang, L.; Liu, Z.; Guo, Q.; Wang, H.; Wang, X.; Dong, X.; Tian, X.; Guo, X. Preparation and Thermal Characterization of Hollow Graphite Fibers/Paraffin Composite Phase Change Material. *Coatings* **2022**, *12*, 160. https://doi.org/10.3390/coatings12020160

Academic Editor: Shih-Chen Shi

Received: 28 December 2021
Accepted: 20 January 2022
Published: 27 January 2022

Publisher's Note: MDPI stays neutral with regard to jurisdictional claims in published maps and institutional affiliations.

Copyright: © 2022 by the authors. Licensee MDPI, Basel, Switzerland. This article is an open access article distributed under the terms and conditions of the Creative Commons Attribution (CC BY) license (https://creativecommons.org/licenses/by/4.0/).

1. Introduction

With the long-term development and utilization of non-renewable resources, the natural environment and human health have been threatened. Therefore, the sustainable development of the society and efficient utilization of clean energy are of concern all over the world [1–7]. Among the renewable energy resources, the thermal energy storage using the phase change material (PCM) has been regarded as an ideal stored energy pattern at the moment [8–14]. PCM can not only be applied at buildings with low energy consumption, but it also serves for fuel cells, lithium ion battery, solar thermoelectric power generation, etc. [15–22]. It can save energy and further improve the efficiency of energy utilization. The corresponding application is attributed to the nature of the PCM. PCM can absorb/release the enormous latent heat with small temperature fluctuation during the melting and solidifying process, which has been used in solar energy utilization, the energy conservation system, and thermal management devices [23–25]. Paraffin wax is a typical kind of PCM, due to its large latent heat, chemic inertness, lack of segregation, and low cost. However, paraffin wax usually exhibits inherent low thermal conductivity, which severely limits its widespread utilization in thermal energy application [26–30].

Different strategies and methods have been used to enhance the thermal properties of the paraffin PCM composite. The thermal conductivity of paraffin can be modified by

adding heat conductive additives. Carbon materials are part of important reinforcements in thermal energy storage [31–33]. Carbon nanotubes have good thermal conductivity. They have a diameter of nanoscale and length of micron scale [34–36]. Paraffin and carbon nanotubes were physically mixed to prepare composition. The composite PCMs displayed good cycle stability when the mass fraction of carbon nanotube was 5%. The thermal conductivity was 0.62 W/(m·K), which was 1.21 times higher than that of pure paraffin [37]. The thermal conductivity of the composite was improved obviously by carbon nanotubes. It is an ideal state in which carbon nanotubes can come into contact in the composites. This can transfer heat quickly throughout the composite PCM. The thermal conductivity of the organic montmorillonite (OMMT)/paraffin/grafted carbon nanotubes composites was 34% higher than that of the OMMT/paraffin composites and 65% higher than that of paraffin [38].

The graphene has the highest thermal conductivity among all of the known materials [39,40]. The defects and oxygen functional groups of the graphene reduce its thermal conductivity. So, it is necessary to anneal the graphene at the high temperature, which can remove the defects and oxygen functional groups [41]. It is beneficial for carbon materials to obtain high thermal conductivity under high-temperature treatment. The thermal performance of paraffin wax PCM can be reinforced obviously by graphene. The thermal conductivity of graphene/paraffin nanocomposite has been improved 66.15% compared with that of pure paraffin with the graphene mass fraction of 2.0 wt% [42].

The expanded graphite can also enhance the thermal property of the paraffin PCM composite. Zhong et al. prepared porous expanded graphite to enhance the thermal property of paraffin wax for latent-heat thermal energy storage [43]. There were many interconnected pores in the expanded graphite, which allowed them to be filled with melted paraffin. The paraffin had more contact areas with ligaments of expanded graphite, which was beneficial to transfer heat throughout the paraffin during the heat transfer process. The experimental results indicated that the natural convection significantly reduced the time necessary for melting.

During the preparation of PCM composites, the nanofillers usually appear aggregation, which results in their uneven distribution throughout the PCM composites and decreasing the heat transfer improvement rate. Therefore, it seems necessary that the fillers should disperse uniformly and form a complete thermal path in the PCM.

Taking the above analysis in mind, the conductive materials should have high thermal conductivity, good corrosion resistance, good dispersibility, and compatibility with PCM. In this work, the hollow graphite fibers (HGFs) are prepared and applied as a thermal conductive material for paraffin. The graphitization was imposed on hollow carbon fibers, optimizing the carbon atom arrangement and lattice order development. The good graphite structure made the HGFs ideal as thermally conductive fillers for paraffin PCM. The successive fiber wall of the HGFs with micron size can form a heat conduction path to transfer heat in paraffin. The HGFs have inner space to accommodate the melted paraffin, which can supply more contact areas with paraffin. Using the vacuum adsorption method, the paraffin PCM composites were fabricated with well-dispersed HGFs and exhibited drastically improved thermal heat flow and heat transfer rate. The thermal conductivity of the HGFs/PCM composite displayed over 680% enhancement as compared with that of the pure PCM (0.32 W/(m·K)), and the corresponding latent conductivity of heat was in the order of 160 J/g. An increase in thermal conductivity of more than 6 times indicates the promising potential application of the HGFs/paraffin PCM on advanced thermal energy storage.

2. Experimental

2.1. Samples Preparation

The hollow graphite fibers (HGFs) were made by melt spinning. The softening point of pitch was 553 K. The pitch was firstly spun into fibers. As-spun fibers were thermo-oxidatively stabilized at 543 K for 0.5 h in oxidation oven under air atmosphere. The

stabilized fibers were carbonized at 1273 K for 0.5 h under nitrogen atmosphere in a tube furnace (Hefei KeJing Material Technology Co., LTD, Hefei, China). The hollow carbon fibers were finally graphitized at 2773 K under argon atmosphere.

The paraffin used in the experiment had a low thermal conductivity of 0.32 W/(m·K), a melting temperature of 333 K, and a latent heat of 219 J/g. The HGFs were mixed with the paraffin, and then heated to 353 K in the vacuum oven for 3 h. Then the composites were allowed to cool until the paraffin wax was solidified under normal atmosphere. Finally, the composites were pressed in a steel module (25 mm × 25 mm × 5 mm).

2.2. Characterization of the Fibers and Composites

The crystallite structure of materials was characterized by an X-ray diffraction system (XRD; D8 advance, Brucker, Karlsruhe, Germany). Field-emission scanning electron microscopy (SEM, JSM-7001F, JEOL, Tokyo, Japan) and field-emission transmission electron microscopy (TEM, JEM-2100F, JEOL, Tokyo, Japan) were used to observe the micro-structure of the samples.

The differential scanning calorimeter (DSC) technique (NETZSCH STA 409PC, Selb, Germany) was applied to measure the latent heat and the phase change temperature of the composite PCMs during the melting and solidifying process with a liquid nitrogen cooling system. The heating and cooling rates of DSC were kept at 2 K·min^{-1}. A thermal gravimetric analyzer (NETSCH TGA 204F1, Selb, Germany) was used to characterize the heat stability of the samples. The thermal conductivity of the composites was calculated by $\lambda = \rho\alpha C_p$, where ρ was density,α was diffusion coefficient and C_p was heat capacity at constant pressure.

3. Results and Discussion

3.1. Hollow Graphite Fibers

According to physical adsorption theory, we prepared the original composite using the hollow pitch fibers, which did not endure a heat treatment process. In order to confirm whether the hollow pitch fibers could form a composite with paraffin or not, the optical microscopy was applied to observe the morphology features. As shown in Figure 1a, the hollow pitch fibers were seen clearly. The three-dimensional stereogram of the original composite was depicted in Figure 1b. The hollow pitch fibers were covered by paraffin, and the hole of the fiber was also partially filled with paraffin. Basing on the above work and the result, the further experimental work was carried out.

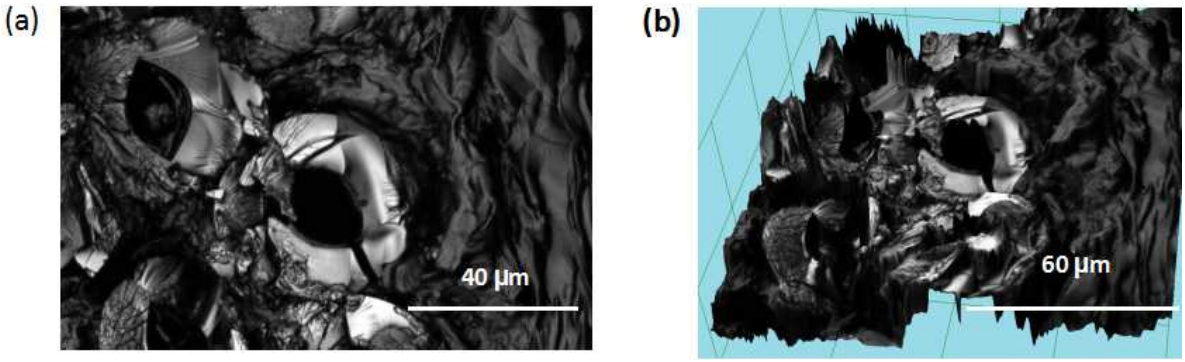


Figure 1. Optical microscopy image of the original composite: Hollow pitch fibers/Paraffin composite (**a**), the three-dimensional stereogram of Hollow pitch fibers/Paraffin composite (**b**).

The HGFs displayed a hollow transverse morphology without any cracking, as shown in Figure 2. The hollow cross structure of the fibers was kept during the whole process from the pitch fibers to the HGFs without any treatment or modification. The average cross-section diameter of the fibers is ca. 40 μm with a hollow degree of 23%. The long

successive hollow structure functions as microscale hollow tube, which permits the liquid or solid materials to infiltrate.



Figure 2. SEM image of the HGFs.

The SEM image of single hollow graphite fiber is depicted in Figure 3a. The hollow space with an oval shape was seen clearly. To disclose a more explicit description of the structure of the HGFs, observation with TEM was carried out, as shown in Figure 3a. It is seen that the orientation of the graphitic basal plane is well ordered in Figure 3b. The electron diffraction pattern taken from the entire area showed clearly a diffraction spot. The graphite layered structure is conductive to heat transfer. Judging from the TEM analysis, the HGFs have good graphite structure, which also indicate the corresponding good electric/thermal conductive property.

The XRD analysis was carried out to investigate the crystal structure of the HGFs, as shown in Figure 3c. The d_{002} of the HGFs was 0.3382 nm, which strongly indicates that HGFs had a good crystalline order. The above structural property endows the HGFs with a good graphite layer to transfer heat. This was also beneficial to promote the heat transfer improvement rate of the prepared composites.

3.2. Hollow Graphite Fibers/Paraffin Composite PCM

The prepared HGFs/paraffin composite PCM was also observed by SEM. The cross section of the composite was showed in Figure 4a. The HGFs were distributed orderly in the paraffin. In addition, the hollow space was continuous along the fiber axis direction, which was filled with paraffin. This is also beneficial to enhance the interface contact between paraffin and the HGFs. TG analyses on the HGFs/paraffin composite as well as pure paraffin are demonstrated in Figure 4b. In the whole process, no main weight loss for paraffin and the HGFs/paraffin composite was observed when the temperature was lower than about 473 K. Then, the HGFs/paraffin composite and paraffin were gradually decomposed with the increase in the temperature.

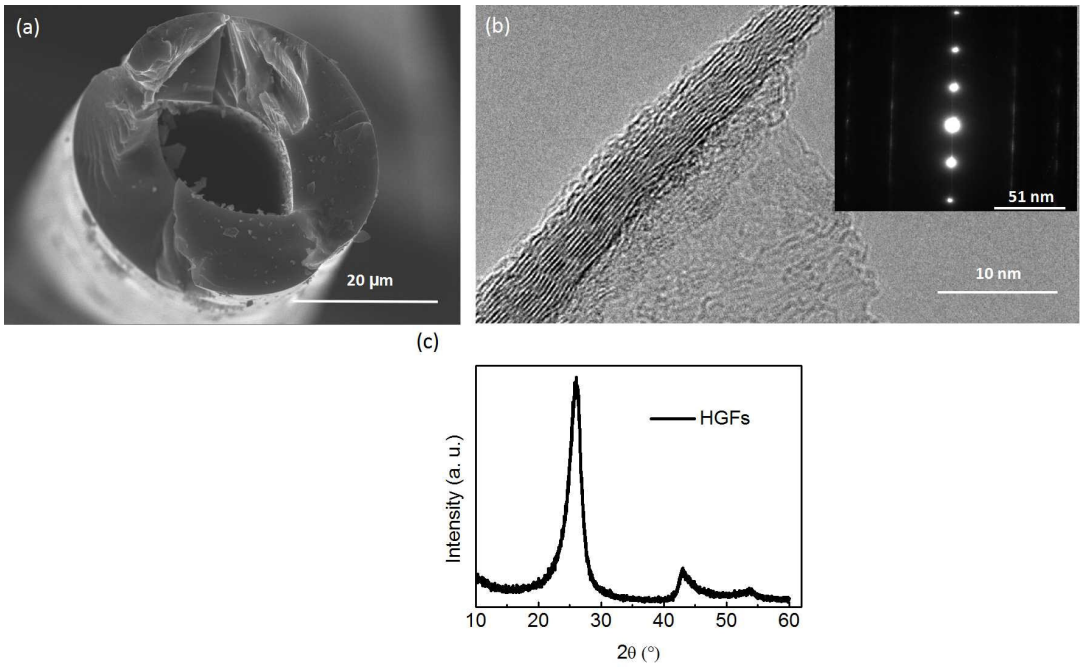


Figure 3. The SEM image of single hollow graphite fiber (**a**). TEM image of the HGFs: ribbons of graphite layer, the inset displays the electron diffraction pattern taken from the entire area (**b**). XRD pattern of the HGFs (**c**).

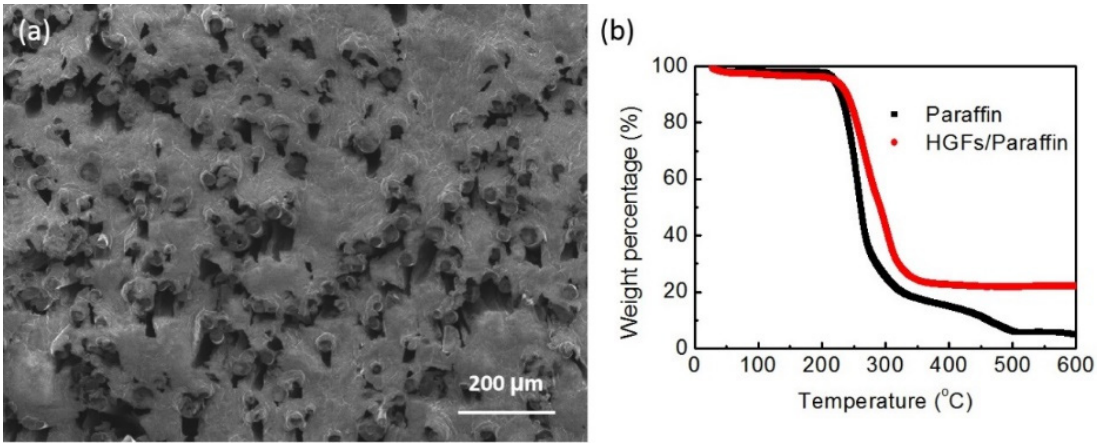


Figure 4. SEM image of the HGFs/Paraffin composite (**a**) and the TGA curves of HGFs/Paraffin wax composite and pure paraffin (**b**).

As one of the graphite materials, the HGFs had certain antioxidant property, which could improve the antioxidant property of the composites. As illustrated in Figure 4b, the loss weight percentage rate of the HGFs/paraffin was lower than that of the pure paraffin with the increase in the temperature. As one kind of graphite material, the HGFs also have good acid and alkali resistance, corrosion resistance, and oxidation resistance. When the paraffin is melted (<100 °C), the stability of the HGFs in the PCM will keep well. There will be no chemical reaction taking place between paraffin and the HGFs.

The thermal conductivity and the latent heat of the composites were tested by DSC and are shown in Figure 5a. The mass loading of the paraffin absorbing along the long successive HGFs was dependent on the vacuum adsorption process. The mass loading of HGFs was increased from 13.36 wt% to 27 wt% in the composites. The fiber wall functioned as a "path" for heat transferring, which allowed the heat to transfer throughout the composite quickly. The thermal conductivity of the HGFs/paraffin composite was

1.51 W/(m·K) along the axial direction of the fiber, and the corresponding thermal conductivity was 0.41 W/(m·K) along the radial direction of the fiber, which contains the HGFs with a mass ratio of 13.36 wt%. With the increase in mass ratio of the HGFs, the thermal conductivity showed an increasing tendency. The corresponding thermal conductivity of the HGFs/paraffin composite along the axial and radial direction of the fiber were 2.50 W/(m·K) and 0.88 W/(m·K), respectively, which was 7.81 times and 2.75 times as much as that of the pure paraffin. The thermal physical data of the composites can be seen in Table S1 of the Supplementary Materials. The results showed that the HGFs effectively gave rise to an improvement in the thermal conductivity of the system. This was ascribed to the good graphite structure and good thermal conductivity of the HGFs. In the HGFs/paraffin composite PCM, the HGFs were long fibers without short cutting, which could supply a good successive heat transfer path. Meanwhile, in the one-dimensional direction, the composites could absorb the heat quickly and not influence other directions seriously. The anisotropic thermal conductivity of the composites could give materials the need to serve in a particular environment.

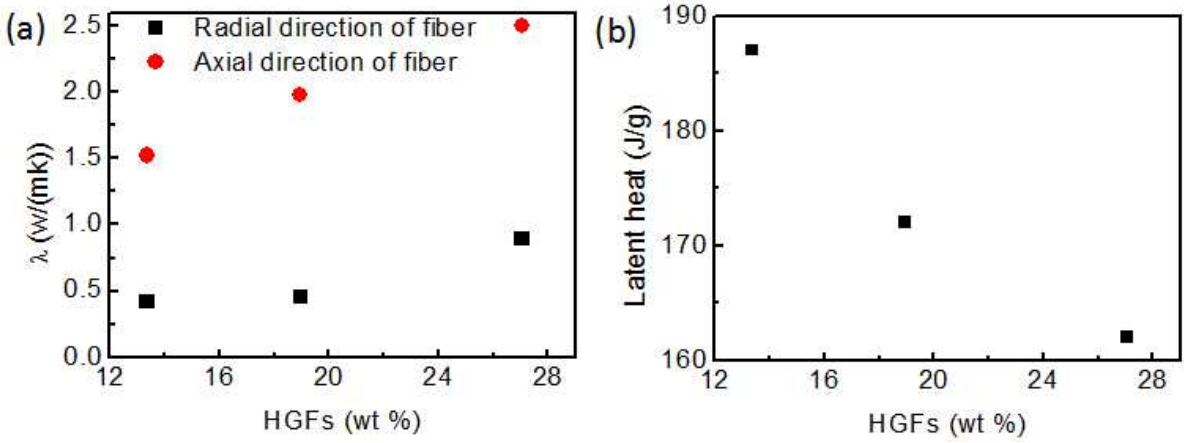


Figure 5. Thermal conductivity (**a**) and latent heat (**b**) of the HGFs/Paraffin composite PCM with mass ratio of the HGFs.

The melted paraffin can be absorbed along the long successive fibers in a vacuum environment. According to the mass ratio of the HGFs in the composite, the latent heats of the composites were 187, 172, and 161 J/K, as shown in Figure 5b. The HGFs occupied the space of the paraffin in the composite, so that the latent heat capacity of the system was lower than that of the pure paraffin. The carbon fibers can be woven into cloth, which can have the potential to prepare the flexible composite PCM.

The melting/solidifying DSC curves of the manufactured HGFs/paraffin composite PCM and pure paraffin are presented in Figure 6. The positive heat flow represents the heat absorbed by the composite PCM during the melting process, whereas the negative heat flow was the heat released during the freezing process. In the melting process, the highest heat flow value of paraffin was 3.01 W/g at 74.23 °C. During the solidifying process, the lowest heat flow value of paraffin was 2.54 W/g at 60.45 °C.

As seen from the DSC curves of the HGFs/paraffin composite PCM, the thermal characteristics of the HGFs/paraffin composite PCM were different from those of the pure paraffin. The heat flow values of the HGFs/paraffin composite PCM were modified by the HGFs. When the HGFs mass fraction in the composite was 18.9 wt%, the temperature of the highest heat flow value of the HGFs/paraffin composite PCM shifted to 71.27 °C, which was lower than that of the paraffin. The corresponding heat flow value of the HGFs/paraffin the composite PCM was raised to 3.738 W/g in the melting cycle, which was 24% higher than that of the paraffin. The existence of the HGFs in paraffin improved the heat flow rate compared with that of the pure paraffin.

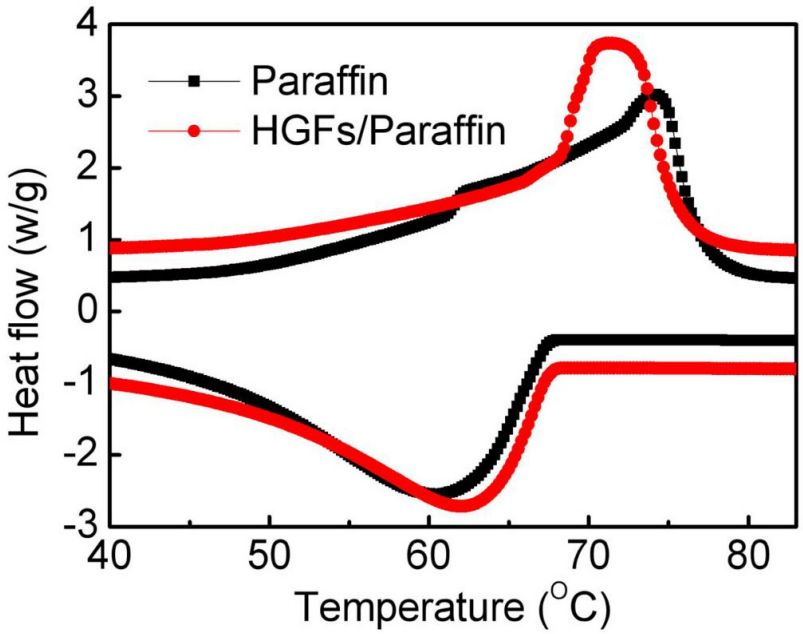


Figure 6. The DSC curves of the paraffin and HGFs/paraffin composite.

During the freezing process, the temperature of the lowest heat flow value of the HGFs/paraffin composite PCM shifted to 61.93 °C. The corresponding heat flow value of the HGFs/paraffin composite PCM was increased to 2.71 W/g. The above results indicated that the HGFs increased the heat flow values of the composite PCM. The HGFs could make the composites release the thermal energy faster in contrast to that of the paraffin. It was obviously that the HGFs/paraffin composite PCM could be applied as thermal energy storage material with good thermal conductivity.

4. Conclusions

In conclusion, the HGFs derived from pitch were prepared as thermal conductive materials. The composite PCM was designed and fabricated by adsorption theory using the vacuum adsorption method. As thermal conductive additives, the HGFs obviously improved the heat flow and heat transfer rate of paraffin PCM. The successive fiber wall supplied a "path" for heat transferring, which allowed the heat transfer throughout the paraffin. When the mass ratio of the HGFs was 27 wt%, the thermal conductivity of the HGFs/paraffin composite PCM along the fiber axis was 2.50 W/(m·K), the corresponding thermal conductivity along the radial direction of fiber axis was 0.88 W/(m·K), which showed 7.81 times and 2.75 times as much as that of the pure paraffin, and the phase change enthalpy maintained at 160 J/g.

It can be concluded that the HGFs/paraffin composite PCM could be applied as a thermal energy storage material. In future work, the HGFs will be prepared to be carbon cloth to fabricate the composite PCM. The composite PCM will be thin and flexible, which will be very meaningful for the energy storage industry.

Supplementary Materials: The following are available online at https://www.mdpi.com/article/10.3390/coatings12020160/s1, Table S1: The thermal physical data of the composites.

Author Contributions: Conceptualization, Z.L., Q.G. and H.W.; methodology, L.W.; software, X.G.; validation, L.W. and Z.L.; formal analysis, L.W.; investigation, L.W. and X.W.; resources, L.W.; data curation, L.W. and X.G.; writing—original draft preparation, L.W., X.D. and Z.L.; writing—review and editing, L.W., X.W. and Z.L.; visualization, X.T.; supervision, H.W.; project administration, L.W.; funding acquisition, H.W. All authors have read and agreed to the published version of the manuscript.

Funding: This work was sponsored by the Project of the China National Natural Science Foundation (No. 21703209, 51666002), the Shanxi Province Science Foundation (No. 201901D211270, 20210302123052), Program for the Outstanding Innovative Teams of Higher Learning Institutions of Shanxi, the Graduate Student Education Innovation Projects of Shanxi Province (No. 2020SY352, 2020SY355), and the Foundation of North University of China (No. 110132).

Institutional Review Board Statement: Not applicable.

Informed Consent Statement: Not applicable.

Data Availability Statement: Data is contained within the article.

Conflicts of Interest: The authors declare no conflict of interest.

References

1. Edwards, L.; Wilkinson, P.; Rutter, G.; Milojevic, A. Health effects in people relocating between environments of differing ambient air pollution concentrations: A literature review. *Environ. Pollut.* **2022**, *292*, 118314. [CrossRef] [PubMed]
2. Ming, Y.; Deng, H.; Wu, X. The negative effect of air pollution on people's pro-environmental behavior. *J. Bus. Res.* **2022**, *142*, 72–87. [CrossRef]
3. Brauer, M.; Casadei, B.; Harrington, R.A.; Kovacs, R.; Sliwa, K.; Brauer, M.; Davaakhuu, N.; Hadley, M.; Kass, D.; Miller, M.; et al. Taking a stand against air pollution—The impact on cardiovascular disease: A joint opinion from the World Heart Federation, American College of Cardiology, American Heart Association, and the European Society of Cardiology. *J. Am. Coll. Cardiol.* **2021**, *77*, 1684–1688. [CrossRef] [PubMed]
4. Güney, T. Solar energy, governance and CO_2 emissions. *Renew. Energy* **2022**, *184*, 791–798. [CrossRef]
5. De Castro, M.; Salvador, S.; Gómez-Gesteira, M.; Costoya, X.; Carvalho, D.; Sanz-Larruga, F.J.; Gimeno, L. Europe, China and the United States: Three different approaches to the development of offshore wind energy. *Renew. Sustain. Energy Rev.* **2019**, *109*, 55–70. [CrossRef]
6. Wu, G.; Zeng, M.; Peng, L.; Liu, X.; Li, B.; Duan, J. China's new energy development: Status, constraints and reforms. *Renew. Sustain. Energy Rev.* **2016**, *53*, 885–896.
7. Kim, C. A review of the deployment programs, impact, and barriers of renewable energy policies in Korea. *Renew. Sustain. Energy Rev.* **2021**, *144*, 110870. [CrossRef]
8. Mahmoud, M.; Ramadan, M.; Olabi, A.-G.; Pullen, K.; Naher, S. A review of mechanical energy storage systems combined with wind and solar applications. *Energy Convers. Manag.* **2020**, *210*, 112670. [CrossRef]
9. Xue, S.; Tan, C.; Kandlakunta, P.; Oksuz, I.; Hlinka, V.; Cao, L.R. Methods for improving the power conversion efficiency of nuclear-voltaic batteries. *Nucl. Instrum. Methods Phys. Res. Sect. A Accel. Spectrom. Detect. Assoc. Equip.* **2019**, *927*, 133–139. [CrossRef]
10. Khezri, R.; Mahmoudi, A.; Aki, H. Optimal planning of solar photovoltaic and battery storage systems for grid-connected residential sector: Review, challenges and new perspectives. *Renew. Sustain. Energy Rev.* **2022**, *153*, 111763. [CrossRef]
11. Yang, Y.; Hoang, M.T.; Bhardwaj, A.; Wilhelm, M.; Mathur, S.; Wang, H. Perovskite solar cells based self-charging power packs: Fundamentals, applications and challenges. *Nano Energy* **2022**, *94*, 106910. [CrossRef]
12. Almoghayer, M.A.; Woolf, D.K.; Kerr, S.; Davies, G. Integration of tidal energy into an island energy system—A case study of Orkney islands. *Energy* **2021**, 122547. [CrossRef]
13. Kumar, A.; Bhattacharya, T.; Mozammil Hasnain, S.M.; Kumar Nayak, A.; Hasnain, M.S. Applications of biomass-derived materials for energy production, conversion, and storage. *Mater. Sci. Energy Technol.* **2020**, *3*, 905–920. [CrossRef]
14. Pachori, H.; Choudhary, T.; Sheorey, T. Significance of thermal energy storage material in solar air heaters. *Mater. Today Proc.* **2022**, in press. [CrossRef]
15. Bendic, V.; Dobrotă, D. Theoretical and experimental contributions on the use of smart composite materials in the construction of civil buildings with low energy consumption. *Energies* **2018**, *11*, 2310. [CrossRef]
16. Bendic, V.; Dobrotă, D.; Dobrescu, T.; Enciu, G.; Pascu, N. Rheological issues of phase change materials obtained by the complex coacervation of butyl stearate in poly methyl methacrylate membranes. *Energies* **2019**, *12*, 917. [CrossRef]
17. Bendic, V.; Dobrotă, D.; Simion, I.; Bălan, E.; Pascu, N.-E.; Tilina, D.I. Methods for determining the thermal transfer in phase-changing materials (PCMs). *Polymers* **2020**, *12*, 467. [CrossRef]
18. Solomon, J.; Kugarajah, V.; Ganesan, P.; Dharmalingam, S. Enhancing power generation by maintaining operating temperature using phase change material for microbial fuel cell application. *J. Environ. Chem. Eng.* **2022**, *10*, 107057. [CrossRef]
19. Gao, Z.; Deng, F.; Yan, D.; Zhu, H.; An, Z.; Sun, P. Thermal performance of thermal management system coupling composite phase change material to water cooling with double s-shaped micro-channels for prismatic lithium-ion battery. *J. Energy Storage* **2022**, *45*, 103490. [CrossRef]
20. Tang, L.-S.; Zhou, Y.-C.; Zhou, L.; Yang, J.; Bai, L.; Bao, R.-Y.; Liu, Z.-Y.; Yang, M.-B.; Yang, W. Double-layered and shape-stabilized phase change materials with enhanced thermal conduction and reversible thermochromism for solar thermoelectric power generation. *Chem. Eng. J.* **2022**, *430*, 132773. [CrossRef]

21. Wang, G.; Yang, Y.; Wang, S. Thermophysical properties analysis of graphene-added phase change materials and evaluation of enhanced heat transfer effect in underwater thermal vehicles. *J. Mol. Liq.* **2021**, 118048. [CrossRef]
22. Yu, C.; Park, J.; Youn, J.R.; Song, Y.S. Integration of form-stable phase change material into pyroelectric energy harvesting system. *Appl. Energy* **2022**, *307*, 118212. [CrossRef]
23. Maher, H.; Rocky, K.A.; Bassiouny, R.; Saha, B.B. Synthesis and thermal characterization of paraffin-based nanocomposites for thermal energy storage applications. *Therm. Sci. Eng. Prog.* **2021**, *22*, 100797. [CrossRef]
24. Paneliya, S.; Khanna, S.; Singh, A.P.; Patel, Y.K.; Vanpariya, A.; Makani, N.H.; Banerjee, R.; Mukhopadhyay, I. Core shell paraffin/silica nanocomposite: A promising phase change material for thermal energy storage. *Renew. Energy* **2021**, *167*, 591–599. [CrossRef]
25. Shen, Z.; Kwon, S.; Lee, H.L.; Toivakka, M.; Oh, K. Cellulose nanofibril/carbon nanotube composite foam-stabilized paraffin phase change material for thermal energy storage and conversion. *Carbohydr. Polym.* **2021**, *273*, 118585. [CrossRef]
26. Wang, X.; Guo, Q.; Wang, J.; Zhong, Y.; Wang, L.; Wei, X.; Liu, L. Thermal conductivity enhancement of form-stable phase-change composites by milling of expanded graphite, micro-capsules and polyethylene. *Renew. Energy* **2013**, *60*, 506–509. [CrossRef]
27. Sharma, A.; Tyagi, V.V.; Chen, C.R.; Buddhi, D. Review on thermal energy storage with phase change materials and applications. *Renew. Sustain. Energy Rev.* **2009**, *13*, 318–345. [CrossRef]
28. Karthik, M.; Faik, A.; D'Aguanno, B. Graphite foam as interpenetrating matrices for phase change paraffin wax: A candidate composite for low temperature thermal energy storage. *Sol. Energy Mater. Sol. Cells* **2017**, *172*, 324–334. [CrossRef]
29. Lin, S.C.; Al-Kayiem, H.H. Evaluation of copper nanoparticles—Paraffin wax compositions for solar thermal energy storage. *Sol. Energy* **2016**, *132*, 267–278. [CrossRef]
30. Liu, X.; Lin, C.; Rao, Z. Diffusion and thermal conductivity of the mixture of paraffin and polystyrene for thermal energy storage: A molecular dynamics study. *J. Energy Inst.* **2017**, *90*, 534–543. [CrossRef]
31. Qiu, L.; Ouyang, Y.; Feng, Y.; Zhang, X. Review on micro/nano phase change materials for solar thermal applications. *Renew. Energy* **2019**, *140*, 513–538. [CrossRef]
32. Luo, X.; Guo, Q.; Li, X.; Tao, Z.; Lei, S.; Liu, J.; Kang, L.; Zheng, D.; Liu, Z. Experimental investigation on a novel phase change material composites coupled with graphite film used for thermal management of lithium-ion batteries. *Renew. Energy* **2020**, *145*, 2046–2055. [CrossRef]
33. Yan, S.; Li, Z.; Liu, X.; Chen, F.; Li, W.; Cheng, J. Energy storage enhancement of paraffin with a solar-absorptive rGO@Ni film in a controllable magnetic field. *Energy Convers. Manag.* **2022**, *251*, 114938. [CrossRef]
34. Atinafu, D.G.; Wi, S.; Yun, B.Y.; Kim, S. Engineering biochar with multiwalled carbon nanotube for efficient phase change material encapsulation and thermal energy storage. *Energy* **2021**, *216*, 119294. [CrossRef]
35. Qian, T.; Li, J.; Feng, W.; Nian, H. Enhanced thermal conductivity of form-stable phase change composite with single-walled carbon nanotubes for thermal energy storage. *Sci. Rep.* **2017**, *7*, 44710. [CrossRef]
36. Li, M.; Chen, M.; Wu, Z. Enhancement in thermal property and mechanical property of phase change microcapsule with modified carbon nanotube. *Appl. Energy* **2014**, *127*, 166–171. [CrossRef]
37. Wang, Y.M.; Ding, Y.F.; Wu, H.J. Performance of paraffin/carbon nanotube composite phase change material. *Mod. Chem. Ind.* **2015**, *35*, 130–134.
38. Li, M.; Guo, Q.; Nutt, S. Carbon nanotube/paraffin/montmorillonite composite phase change material for thermal energy storage. *Sol. Energy* **2017**, *146*, 1–7. [CrossRef]
39. Balandin, A.A. Thermal properties of graphene and nanostructured carbon materials. *Nat. Mater.* **2011**, *10*, 569–581. [CrossRef]
40. Balandin, A.A.; Ghosh, S.; Bao, W.; Calizo, I.; Teweldebrhan, D.; Miao, F.; Lau, C.N. Superior thermal conductivity of single-layer graphene. *Nano Lett.* **2008**, *8*, 902–907. [CrossRef]
41. Xin, G.; Sun, H.; Scott, S.M.; Yao, T.; Lu, F.; Shao, D.; Hu, T.; Wang, G.; Ran, G.; Lian, J. Advanced phase change composite by thermally annealed defect-free graphene for thermal energy storage. *ACS Appl. Mater. Interfaces* **2014**, *6*, 15262–15271. [CrossRef] [PubMed]
42. Kumar, K.; Sharma, K.; Verma, S.; Upadhyay, N. Experimental investigation of graphene-paraffin wax nanocomposites for thermal energy storage. *Mater. Today Proc.* **2019**, *18*, 5158–5163. [CrossRef]
43. Zhong, Y.; Li, S.; Wei, X.; Liu, Z.; Guo, Q.; Shi, J.; Liu, L. Heat transfer enhancement of paraffin wax using compressed expanded natural graphite for thermal energy storage. *Carbon* **2010**, *48*, 300–304. [CrossRef]